

Non-Euclidean Erdős–Anning Theorems

David Eppstein*

February 25, 2025

Abstract

The Erdős–Anning theorem states that every point set in the Euclidean plane with integer distances must be either collinear or finite. More strongly, for any (non-degenerate) triangle of diameter δ , at most $O(\delta^2)$ points can have integer distances from all three triangle vertices. We prove the same results for any strictly convex distance function on the plane, and analogous results for every two-dimensional complete Riemannian manifold of bounded genus and for geodesic distance on the boundary of every three-dimensional Euclidean convex set. As a consequence, we resolve a 1983 question of Richard Guy on the equilateral dimension of Riemannian manifolds. Our proofs are based on the properties of additively weighted Voronoi diagrams of these distances.

1 Introduction

Many incidence properties of lines or curves, seemingly mysterious on their own, become obvious when viewed through the lens of computational geometry, where the curves may be features of Voronoi diagrams or related constructions. Thus, for instance, to see that the three perpendicular bisectors of a triangle’s sides meet at a single point, observe that these bisectors contain the edges of the Voronoi diagram of the triangle vertices, and these Voronoi edges meet at the Voronoi vertex. In this work we apply the same principle to the Erdős–Anning theorem on integer distances in the plane, conventionally proven using the algebraic intersection properties of hyperbolae. By reinterpreting these hyperbolae and their intersection points as the cell boundaries and vertices of additively-weighted Voronoi diagrams, and by analyzing these diagrams geometrically and topologically rather than algebraically, we greatly generalize this theorem, to several wide classes of two-dimensional metric spaces. In doing so, we resolve a 1983 question of Richard Guy on the equilateral dimension of Riemannian manifolds, the maximum number of points that can be placed at equal distances from each other in these spaces.

The Erdős–Anning theorem states that every point set in the Euclidean plane with integer distances must be either collinear or finite [1, 11]. More strongly, for any (non-degenerate) triangle of diameter δ , at most $O(\delta^2)$ points can have integer distances from all three triangle vertices. When the whole point set has diameter D , its number of points is $O(D)$ [30], and if in addition it is non-collinear its number of points is $D^{O(1/\log \log D)}$ [13]. In contrast, as Euler already observed, there exist infinite non-collinear point sets of bounded diameter with all distances rational, for instance, dense subsets of a unit circle [12, 15].

There are many metrics other than Euclidean distance for which we might ask similar questions. One obstacle to generalizing the Erdős–Anning theorem to other metrics is that its usual proof is heavily based on algebraic geometry. In the Euclidean plane, the locus of points whose distances

*Department of Computer Science, University of California, Irvine. Donald Bren Hall, Irvine, CA 92697, USA. eppstein@uci.edu.

to two given points differ by a fixed integer is a branch of a hyperbola. Therefore, the points with integer distances to three non-collinear points lie at the intersection points of two finite families of hyperbolas. Hyperbolas are algebraic curves of degree two, and by Bezout's theorem two hyperbolas have at most four crossings, so these two finite families have finitely many intersection points. But it is not obvious how to extend this argument to metrics for which the corresponding curves are more complicated or non-algebraic. Erdős and Anning originally used a different argument using trigonometric inequalities [1], but its generalization is also non-obvious.

A second obstacle is that analogous statements are untrue for some metrics. For the L_1 or L_∞ distances in the plane, the integer lattice provides a familiar example of an infinite set that is not collinear and has only integer distances. Thus, generalizations of the theorem to other families of metrics must avoid families that include L_1 or L_∞ .

In this paper we prove the following generalized versions of the Erdős–Anning theorem:

For any strictly convex distance function on \mathbb{R}^2 , every point set with integer distances must be either collinear or finite. For any (non-degenerate) triangle of diameter δ , at most $O(\delta^2)$ points can have integer distances from all three triangle vertices. If a set with integer distances has diameter D , it has at most $O(D)$ points. (Section 3)

For any two-dimensional complete Riemannian manifold of finite genus g , every point set with integer distances must either be finite or be contained in a geodesic (a locally-shortest curve) that contains every shortest curve between pairs of the points. If some three points do not lie on a single shortest curve, and have diameter δ , at most $O((g+1)\delta^2)$ points can have integer distances from these three points. (Section 4)

For geodesic distance on the boundary of a convex set in \mathbb{R}^3 , every point set with integer distances must either be finite or be contained in a geodesic that contains every shortest curve between pairs of the points. If some three points do not lie on a single shortest curve, and have diameter δ , at most $O(\delta^2)$ points can have integer distances from these three points. If a set with integer distances has diameter D , it has at most $O(D^{4/3})$ points. (Section 5)

Our proofs replace the intersection properties of low-degree algebraic curves with the geometric and topological properties of additively weighted Voronoi diagrams. Our results for Riemannian manifolds resolve a question posed in 1983 by Richard Guy [14], on the *equilateral dimension* of Riemannian manifolds, the maximum number of points at unit distance from each other in these manifolds. Guy asked whether the equilateral dimension could be bounded by a function of dimension. For complete Riemannian 2-manifolds of bounded genus, we bound the equilateral dimension by a function of the genus (Corollary 20) but for locally Euclidean incomplete Riemannian 2-manifolds, for complete Riemannian 2-manifolds of unbounded genus, and for complete Riemannian metrics on \mathbb{R}^3 , we show that the equilateral dimension is unbounded (Example 6 and Example 7).

2 Preliminaries: Voronoi diagrams and star-shaped cells

A *Voronoi diagram* of a finite set of point *sites* in a metric space (X, d) subdivides the space according to which site is closest. Each site s_i has a (closed) cell V_i associated with it, where

$$V_i = \left\{ p \in X \mid d(p, s_i) \leq \min_{j \neq i} d(p, s_j) \right\}$$

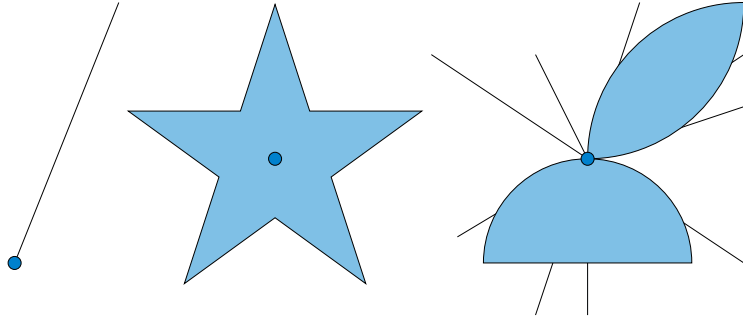


Figure 1: Three star-shaped sets, each shown with a point in its kernel.

is the set of points whose distance to site s_i is less than or equal to the distance to any other site s_j . We will only use Voronoi diagrams of finite sets (in fact, of at most three sites), so we only define and discuss the properties of these diagrams for finite sets of sites.

The intersection of any collection of Voronoi cells is the locus of points having equal distances to their sites. When X has the topology of the plane, the *bisector* of a pair of sites (the intersection of their Voronoi cells) is often (but not always) a curve, and a non-empty intersection of three or more sites is often (but not always) an isolated point or points, called *Voronoi vertices*. We will use *additively weighted* Voronoi diagrams, in which each site s_i has a weight w_i associated with it, and in which the distances in the definition of cells are modified by adding these weights:

$$V_i = \left\{ p \in X \mid d(p, s_i) + w_i \leq \min_{j \neq i} d(p, s_j) + w_j \right\}.$$

Voronoi diagrams have been the object of intensive study, including Voronoi diagrams for convex distance functions [7, 17, 21], for points on a sphere [3, 25, 27], for points in the hyperbolic plane [4, 9, 29], orbifolds [24], and for more general Riemannian manifolds [22]. Additively weighted Voronoi diagrams are also a standard concept [6, 18], and confusingly, are sometimes called *hyperbolic Dirichlet tessellations* despite their use of Euclidean distance [2], because their cells are bounded by hyperbolas (the same hyperbolas from the Erdős–Anning proof). We did not find works combining additive weights and non-Euclidean distances.

The *kernel* of a subset S of the plane is defined as the set of points p such that, for every point q in S , the line segment pq belongs to S . S is convex if and only if its kernel coincides with S . Weakening this formulation of convexity, S is defined to be *star-shaped* if its kernel is non-empty. (See Fig. 1. Note that, according to this definition, star-shaped sets are not required to form topological disks, and the empty set is not star-shaped.) It is known that, for instance, the Voronoi cells of unweighted convex distance functions are star-shaped topological disks [7]. For additively weighted Voronoi diagrams, we should be a little more careful, because of the possibility that a Voronoi cell can degenerate to a line segment, a single point, or the empty set, but in the Euclidean case they are again known to be star-shaped when non-empty [2].

3 Convex distance functions

A *convex distance function* on \mathbb{R}^d can be defined from any centrally symmetric compact convex body K . The resulting function $d_K(p, q)$ is the smallest scale factor s such that a copy of K , scaled by s and centered at p , contains q . Any convex distance function defines a norm on \mathbb{R}^d , $\|p\|_K = d_K(0, p)$. In the reverse direction, the closed unit ball $\{p \mid \|p\| \leq 1\}$ of any norm $\|\cdot\|$ can

be used to define a convex distance function. A convex set is *strictly convex* if its boundary does not contain any line segment, and a *strictly convex distance function* is a convex distance function defined from a strictly convex set. Convex distance functions obey all the requirements of a metric space, including the triangle inequality. For strictly convex distance functions and non-collinear triples of points p, q, r , they obey a strict form of the triangle inequality [7]:

$$d_K(p, r) < d_K(p, q) + d_K(q, r).$$

Examples of strictly convex distance functions include the Minkowski L_p distances for $1 < p < \infty$, obtained from the convex body

$$K_p = \left\{ (x_1, x_2, \dots, x_d) \mid \sum_{i=1}^d x_i^p \leq 1 \right\}.$$

For $p = 1$ and for the limiting case $p = \infty$ one obtains distance functions that are convex but not strictly convex. For $p = 2$ we recover the familiar Euclidean distance.

A *curve*, in one of these spaces, is just a continuous function from the unit interval $[0, 1]$ to the space. Its *endpoints* are the values of this function at 0 and 1. If C is a curve for a space with distance d , we may define its length as

$$\lim_{n \rightarrow \infty} \sum_{i=1}^n d\left(C\left(\frac{i-1}{n}\right), C\left(\frac{i}{n}\right)\right),$$

when this limit exists. Convex distance functions define *geodesic metric spaces* in which the distance between any two points equals the length of a shortest curve between the points. For strictly convex distance functions, this shortest curve is unique: it is just the *line segment* between its two points. It is convenient to combine these observations about shortest curves with the triangle inequality to obtain the following observation about distances:

Observation 1 (Lipschitz property of distances). *Let p, q , and r be points of a geodesic space with distance d , and let C be a curve with endpoints q and r , of length ℓ . Then*

$$-\ell \leq d(p, q) - d(p, r) \leq \ell,$$

with equality on the left side only when C traces without backtracking a subset of a shortest curve from p to r , and with equality on the right side only when C traces without backtracking a subset of a shortest curve from q to p .

Thus, when the space is given by a strictly convex distance function, and when the difference of distances equals the length of the curve C , the three points p, q , and r must be collinear, and curve C must form a segment of their line.

3.1 Examples

In this section we provide examples of integer distance sets for different convex distance functions.

Example 1. The integer grid $\{(x, y) \mid x, y \in \mathbb{Z}\}$ has integer distances for the L_1 distance (the sum of absolute differences of coordinates) and L_∞ distance (maximum absolute difference of coordinates); see Fig. 2. Both the L_1 and L_∞ distance are convex distance functions, but are not strictly convex distance functions. The unit ball of the L_1 distance is a 45° -rotated square with vertices $(0, \pm 1)$ and $(\pm 1, 0)$, while the unit ball of L_∞ distance is an axis-parallel square with vertices $(\pm 1, \pm 1)$.

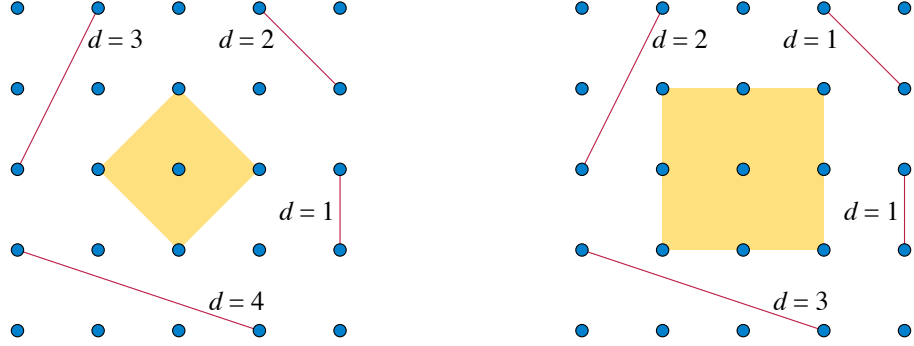


Figure 2: Integer L_1 (left) and L_∞ distances in the integer grid (Example 1). The yellow shaded regions are the unit balls for these two distances.

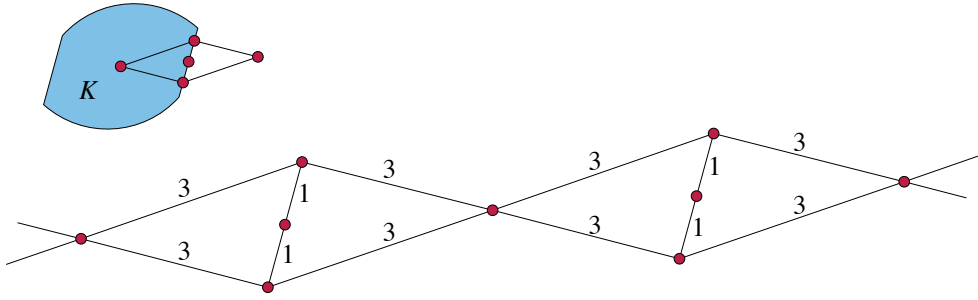


Figure 3: Construction for an infinite non-geodesic set with integer distances for a convex but not strictly convex distance function d_K (Example 3).

Example 2. Let S be any finite set of points in the plane for which all $\binom{n}{2}$ lines determined by S have distinct slopes. Then there exists a strictly convex distance function d_K that assigns integer distances to each pair of points in S . To construct d_K , consider the system of unit vectors obtained by normalizing the vector differences of each pair of points; these form a centrally symmetric set on the unit circle, and by assumption they are distinct. Let ε be a sufficiently small number that expanding any subset of these unit vectors by a factor of $1 + \varepsilon$ would preserve the strict convex position of all the vectors. Scale the unit circle and the vectors on it so that, when using the result as the unit ball for a convex distance function, all distances in S become larger than $1/\varepsilon$. Round each of these distances down to an integer, and expand each of the corresponding vectors by the same factor (at most $1 + \varepsilon$) by which its distance was decreased. Construct K as any strictly convex set through the resulting vectors, for instance by connecting them in cyclic order using circular arcs of sufficiently large radius. Then for this choice of K , each distance in S becomes its rounded value, which by construction is an integer.

A similar construction shows that any countable set of points for which all lines have distinct slopes can be made to have rational (but not integer) distances for a strictly convex distance function, obtained by adding the points one at a time and perturbing the distance function for each added point without changing the previous distances.

Example 3. For any convex distance functions d_K that is not strict, there exist infinite sets that have integer distances but that do not belong to a single shortest curve. To construct such a set, note that if d_K is convex but not strictly convex, then the boundary of K contains a line segment. Place two or more points along this segment, at equal rational distances δ according to d_K , and

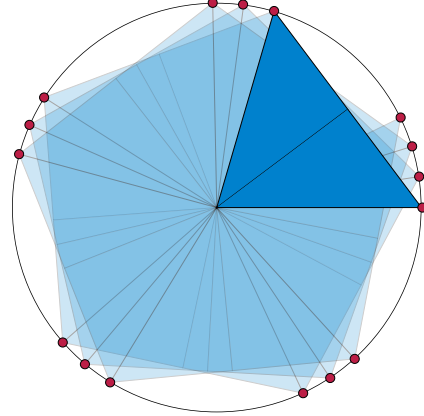


Figure 4: The points on the unit sphere whose angles are even multiples of the angles of a 3-4-5 right triangle have pairwise rational distances.

add two more points at the origin and at its reflection across this line segment, each having unit distance to the entire line segment according to d_K . Scale this system of points by the denominator of δ to produce a finite set of points with integer distances, having a parallelogram as its convex hull. Connecting multiple translated copies of this parallelogram by identifying their copies of the origin and its reflection (Fig. 3) produces the desired infinite non-geodesic set with integer distances.

Example 4. Euclidean distance is a convex distance function, and there exist infinite dense sets of points on the unit circle with rational Euclidean distances [12, 15]. One construction for such a system of points uses complex number coordinates for the points of the plane, and consists of the complex numbers $\{q^{2j} \mid j \in \mathbb{Z}\}$ where $q = \frac{a}{c} + i\frac{b}{c}$ is a rational point on the unit circle derived from an integer right triangle with side lengths a , b , and c . Geometrically, this point set is obtained from a single point by repeatedly rotating by twice the angle of the triangle.¹ Fig. 4 shows an example derived from the 3-4-5 right triangle. Arbitrarily large finite non-collinear point sets at integer distances can be obtained by taking a finite subset of this infinite set (possibly including also the center of the circle) and scaling it to clear the denominators in its coordinates.

It is an open problem whether there exist arbitrarily-large sets of points at integer Euclidean distances that have no three points in a line and no four points on a circle [10]. The largest such sets known have only seven points [19, 20].

3.2 Degenerate and non-degenerate sites

In unweighted Voronoi diagrams, every cell is a topological disk (or the whole space), having its site in its interior. That is not true for additively weighted Voronoi diagrams, but the cells that do not have their site in their interior have a very special structure, which we examine in this section.

Lemma 2. *For additively weighted Voronoi diagrams of 2-dimensional strictly convex distance functions, every non-empty Voronoi cell is star-shaped with its site in its kernel.*

Proof. The star-shaped property is an immediate consequence of the Lipschitz property of distances. If site s_i has the minimum weighted distance to a given point p , then for any other point q on line

¹This construction is essentially due to Harborth [15] but he states it incorrectly as using all integer multiples of the angle rather than only the even multiples.



Figure 5: An additively weighted Voronoi diagram with two degenerate sites (red and green) and two non-degenerate sites (yellow and blue). The red site has equal weighted distance to itself and to the yellow site; its Voronoi cell (shown as a red line segment) extends along a ray, away from the yellow site, to the boundary of the yellow Voronoi cell. The green site has larger weighted distance to itself than to the blue site, so its Voronoi cell is empty. The Voronoi cells for the yellow and blue sites together cover the plane, separated from each other by the central vertical line. The distance function is unspecified; it could be Euclidean, or any other strictly convex distance function whose unit disk has vertical reflection symmetry (so that the bisector of the two horizontally-aligned yellow and blue points is a vertical line).

segment ps_i , the weighted distance from s_i to q is less by $d(p, q)$, while other weighted distances decrease by at most the same amount, so the weighted distance from s_i remains minimum. Thus, if p belongs to the Voronoi cell of s_i , so does every point q on line segment ps_i . \square

Definition 1. Define a *degenerate site* of an additively weighted Voronoi diagram of a 2-dimensional strictly convex distance function to be a site that belongs to the Voronoi cell of another site. Define a *non-degenerate site* to be a site that is not degenerate.

For examples of degenerate and non-degenerate sites, see Fig. 5. The next lemma explains the shapes of the cells in this example:

Lemma 3. *Let s_i be a degenerate site of an additively weighted Voronoi diagram of a 2-dimensional strictly convex distance function, with s_i belonging to the Voronoi cell V_j of another site s_j . Let R be a ray on line $s_i s_j$ with s_i as its initial point, extending away from s_j . Then either s_i is empty, or $V_i = R \cap V_j$.*

Proof. If the weighted distance from s_i to s_j is less than the weighted distance from s_i to itself, then s_i does not belong to its own Voronoi cell, and the only possibility according to Lemma 2 is that V_i is empty. Otherwise, at s_i , the weighted distances to s_i and s_j are equal. Let R be as described in the statement of the lemma. By the Lipschitz property of distances, every point of R has equal weighted distance to s_i and to s_j , and every other point in the plane has smaller weighted distance to s_j than to s_i . Therefore, the set of points whose weighted distance to s_i is minimum (among weighted distances to all sites) is exactly $R \cap V_j$. \square

By repeatedly using Lemma 3 to replace the Voronoi cells of degenerate sites with supersets that are also Voronoi cells, until no more such replacements can be performed, we obtain:

Corollary 4. *In an additively weighted Voronoi diagram of a 2-dimensional strictly convex distance function, every point belongs to the Voronoi cell of at least one non-degenerate site.*

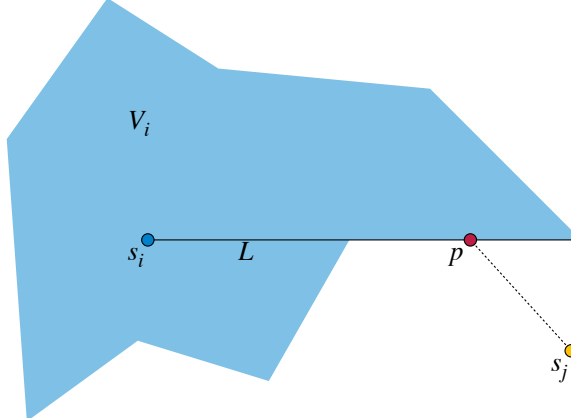


Figure 6: Figure for the proof of Lemma 6: a site s_i , a segment L within Voronoi cell V_i , and a point p in the relative interior of L that is not interior to V_i . The lemma proves that this situation cannot exist by considering cases for the location of s_j , another site with the same distance to p as s_i .

Note that Corollary 4 would not be true if we allowed infinite sets of sites. Instead of defining degeneracy of a site by its membership in other cells, we have an equivalent characterization by its position within its own cell:

Lemma 5. *A site s_i of an additively weighted Voronoi diagram of a 2-dimensional strictly convex distance function is non-degenerate if and only if it is an interior point of its cell V_i .*

Proof. If s_i is an interior point of V_i , V_i cannot be a subset of a ray (which has no interior points), and it follows from Lemma 3 that s_i is non-degenerate. If s_i is not an interior point of V_i , then every neighborhood of s_i has points that are not in V_i , and therefore there exists some other cell V_j intersecting this neighborhood. Because there are only finitely many sites, we can reverse the quantifiers: there exists some other cell V_j that intersects every neighborhood of s_i . But because cells are closed sets, this implies that $s_i \in V_j$ and s_i is degenerate. \square

As the next lemma shows, each ray with a non-degenerate site as its initial point passes through at most one boundary point of its Voronoi cell.

Lemma 6. *Let s_i be a non-degenerate site of an additively weighted Voronoi diagram of a 2-dimensional strictly convex distance function, let L be a line segment in V_i having s_i as an endpoint, and let p be a point in the relative interior of L . Then p is interior to V_i .*

Proof. Suppose for a contradiction that p is not interior to V_i . Then by finiteness of the number of sites, there must exist another site s_j such that every neighborhood of p contains points of $V_j \setminus V_i$. Because Voronoi cells are closed, p belongs to V_j as well as to V_i , and has equal weighted distance to s_i and s_j . We now distinguish three cases for the possible location of s_j :

- Suppose that s_j does not lie on the line containing L , as shown in Fig. 6, or lies on the opposite side from p as s_i on this line or great circle. Then by the Lipschitz property of distances, all points of L that are on the opposite side from p as s_i would have smaller weighted distance to s_j than to s_i , because the distance from s_i increases at the same rate as distance from p along L , while the distance from s_j cannot increase as quickly. But this contradicts the assumption that some of these points belong to V_i .

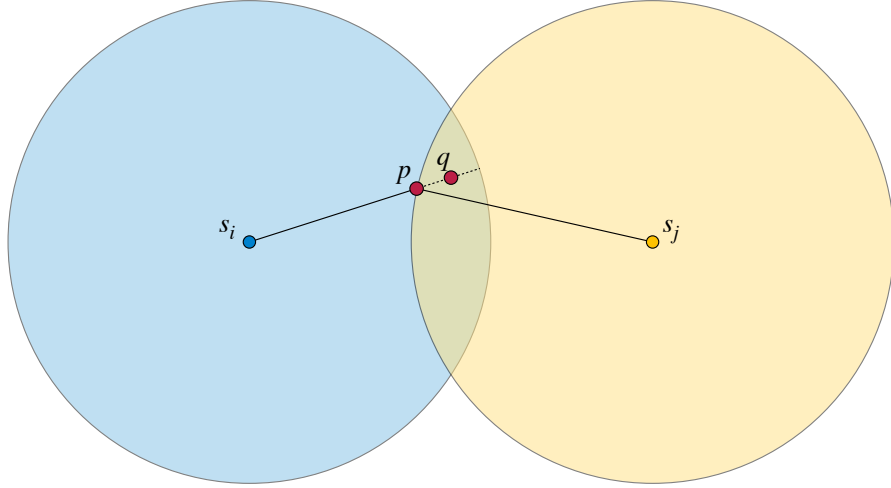


Figure 7: Figure for the proof of Lemma 7: if a point p could belong to the interior of the Voronoi cell V_i for non-degenerate site s_i , and also belong to the Voronoi cell for s_j , then some point q past p on the same ray would also belong to V_i , contradicting the Lipschitz property of distances.

- Suppose that s_j lies on segment or arc ps_i . Then $s_j \in V_i$, and by Lemma 3 its Voronoi cell V_j is a subset of V_i , contradicting the assumption that N contains a point of $V_j \setminus V_i$.
- The only remaining case is that s_i lies on line segment ps_j . But this lies within V_j by Lemma 2, so $s_i \in V_j$, contradicting the assumption that s_i is non-degenerate.

As all cases lead to a contradiction, the assumption that p is not interior to V_i must be false. \square

3.3 Intersections of non-degenerate cells

In Section 3.2, we studied the shapes of individual cells of additively weighted Voronoi diagrams. In this section we instead consider the intersection patterns of cells.

Lemma 7. *Let s_i and s_j be non-degenerate sites of an additively weighted Voronoi diagram for a 2-dimensional strictly convex distance function. Then the interior of V_i is disjoint from V_j , and vice versa.*

Proof. Suppose for a contradiction that there existed a point p interior to V_i that also belonged to V_j . Then segments ps_i and ps_j must be disjoint except for their shared endpoint, for otherwise one would be a subset of the other, and one of the two sites would belong to the Voronoi cell of the other, contradicting the assumption that both are non-degenerate. Because p belongs to both V_i and V_j , it has equal weighted distance to both sites. Because p is interior to V_i , we can extend line segment ps_i within a neighborhood of p inside V_i , to obtain a line segment qs_i that still remains entirely interior to V_i (Fig. 7). By the Lipschitz property of distances, q is farther than p from s_i by an amount equal to the distance from p to q , while the distance from q to s_j cannot increase as quickly. Therefore, q belongs to the Voronoi diagram of V_j but not of V_i , contradicting our construction of q as a point in V_i . This contradiction shows that our assumption of a point interior to V_i and in V_j cannot hold: no such point exists. Symmetrically, no point interior to V_j can also belong to V_i . \square

Lemma 8. *Let s_i and s_j be distinct non-degenerate sites of an additively weighted Voronoi diagram of a 2-dimensional strictly convex distance function, and let p and q be distinct points of V_i and V_j respectively. Then line segments (or arcs) ps_i and qs_j are disjoint.*

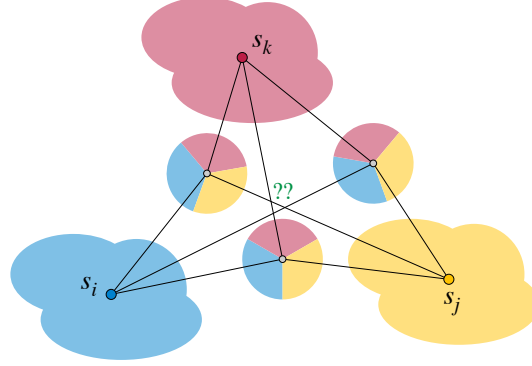


Figure 8: Figure for the proof of Lemma 9: Three non-degenerate sites s_i , s_j , and s_k , and three points belonging to the intersection of Voronoi cells $V_i \cap V_j \cap V_k$, would form a drawing of the non-planar graph $K_{3,3}$.

Proof. Otherwise, one of these two segments would contain a point in the relative interior of the other segment or arc. By Lemma 6 this point would be interior to its Voronoi cell, contradicting Lemma 7. \square

Finally, we consider intersections of three Voronoi cells, in the main lemma needed for our proof of our non-Euclidean Erdős–Anning theorem:

Lemma 9. *Let s_i , s_j , and s_k be non-collinear sites of an additively weighted Voronoi diagram of a 2-dimensional strictly convex distance function. Then $V_i \cap V_j \cap V_k$ consists of at most two points.*

Proof. Without loss of generality we may consider that these are the only three sites of the Voronoi diagram, because adding more sites can only reduce the points in $V_i \cap V_j \cap V_k$ by causing some of those points to belong to Voronoi cells of other sites. By Lemma 6 and Lemma 7, the whole space is covered by the cells of non-degenerate sites, with disjoint interiors. We distinguish cases by how many of the three given sites are non-degenerate:

- Suppose that there is only one non-degenerate site, without loss of generality s_i . Then, V_i is the whole space, and V_j and V_k lie on rays extending away from s_i . These rays diverge from each other (by non-collinearity) and must be disjoint, so $|V_i \cap V_j \cap V_k| = 0$.
- In the next case, there are two non-degenerate sites, without loss of generality s_i and s_j . Because it is degenerate, s_k belongs to at least one of their Voronoi cells, without loss of generality V_i . By Lemma 3, V_k has the form $R \cap V_i$, where R is a ray collinear with s_i . By Lemma 6, only the farthest point from s_i on $R \cap V_i$ can be a boundary point of V_i ; all the other points are interior to V_i . By Lemma 7, only the one boundary point can also belong to V_j . Thus, in this case, $|V_i \cap V_j \cap V_k| \leq 1$ again.
- In the remaining case, all three sites are non-degenerate. In particular, none of them belong to $V_i \cap V_j \cap V_k$. Consider the system of line segments connecting each site to each point of $V_i \cap V_j \cap V_k$. By Lemma 8 these line segments cannot intersect except at shared endpoints, so they form a planar drawing of a complete bipartite graph with the three sites on one side of its bipartition and the points of $V_i \cap V_j \cap V_k$ on the other side. If there could be three points in $V_i \cap V_j \cap V_k$, this would give a planar drawing of $K_{3,3}$, a non-planar graph (Fig. 8). Therefore, $|V_i \cap V_j \cap V_k| \leq 2$. \square

3.4 Erdős–Anning theorems for strict convex distance functions

Theorem 1. *Let s_1 , s_2 , and s_3 be three non-collinear points of a 2-dimensional strictly convex distance function d . Then the number of points that can have integer distances to all three of s_1 , s_2 , and s_3 is $O(d(s_1, s_2) \cdot d(s_1, s_3))$.*

Proof. Let p be a point with integer distances to all three of s_1 , s_2 , and s_3 . Consider the additively weighted Voronoi diagram of these three sites, with weights $w_i = d(s_i, p) - d(s_i, p)$. Then at p , the three additively weighted distances all equal $d(s_i, p)$, so all three sites are equal nearest neighbors. This means that p must belong to the triple intersection of Voronoi cells $V_1 \cap V_2 \cap V_3$.

Weight w_1 is identically zero, and by the triangle inequality the remaining two weights have absolute values $|d(s_1, p) - d(s_2, p)|$ and $|d(s_1, p) - d(s_3, p)|$ that are at most $d(s_1, s_2)$ and $d(s_1, s_3)$ respectively. Therefore, there are at most $(2d(s_1, s_2) + 1) \cdot (2d(s_1, s_3) + 1)$ combinations of weights defining an additively weighted Voronoi diagram for which p might be a triple intersection point, and at most two triple intersection points per diagram by Lemma 9, giving a total of at most $2(2d(s_1, s_2) + 1) \cdot (2d(s_1, s_3) + 1)$ possible points that can have integer distances to all three of s_1 , s_2 , and s_3 . \square

The following generalization of the Erdős–Anning theorem follows immediately:

Theorem 2. *If a set S of points of a 2-dimensional strictly convex distance function has the property that all distances between points of S are integers, then S is finite or collinear.*

Proof. If S is not collinear, it has three non-collinear points to which we apply Theorem 1. \square

3.5 Diameter bounds

The number of points in a set with integer distances can also be bounded linearly in the diameter of the set, generalizing a result of Solymosi [30] for Euclidean distance.

Theorem 3. *If a set S of points of a 2-dimensional strictly convex distance function has diameter D (measured according to that distance function), and all distances in S are integers, then $|S| = O(D)$, with a constant of proportionality that depends on the distance function.*

Proof. We may assume without loss of generality that the unit ball of the given distance function d is contained in a Euclidean unit circle. For, if it does not, let ξ be the maximum Euclidean distance from the origin to any point of the unit d -ball, and scale both S and d by $1/\xi$, leaving distances between the scaled points unchanged and allowing the d -ball to fit within a Euclidean unit circle. Let ρ be the minimum Euclidean distance from the origin of the unit circle of d ; note that, if we treat the distance function as fixed, then ρ is a constant. Then the function measured by d is lower bounded by the Euclidean distance, and upper bounded by $\frac{1}{\rho}$ times the Euclidean distance. From the lower bound on d , the Euclidean diameter of S is at most its d -diameter, D .

Enclose S in a square bounding box of (Euclidean) side length D , and center this within a larger square B of side length $3D$, so that all points of S are at Euclidean distance at least D from the boundary of B . Construct the (Euclidean) Voronoi diagram of S , and let s_1 be the point of S whose Voronoi cell V_1 , intersected with B , has the smallest Euclidean area, $\leq 9D^2/n = O(D^2/n)$. Let s_2 be the Euclidean nearest neighbor of s_1 in S , let m be the midpoint of s_1 and s_2 , and construct a right triangle ps_1m with right angle at s_1 , contained in $V_1 \cap B$, with the largest possible Euclidean area. (See Fig. 9 for an example.) We distinguish two cases:

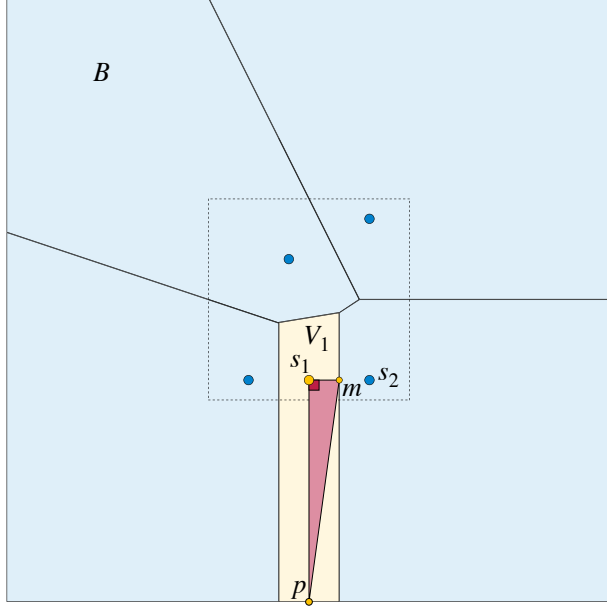


Figure 9: Figure for the proof of Theorem 3: After enclosing the given points in a bounding box B of side length three times the diameter D , s_1 is the point whose Euclidean Voronoi cell V_1 has the smallest intersection with B , s_2 is its nearest neighbor, m is their midpoint, and right triangle ps_1m is chosen to have as large an area as possible within $V_1 \cap B$. In the case shown, p is on the boundary of B , at distance greater than D from s_1 , from which it follows that $d(s_1, s_2) = O(D/n)$.

- If p is on the boundary of B , as shown in Fig. 9, it is at Euclidean distance $\geq D$ from s_1 . In order for right triangle ps_1s_2 to have area $O(D^2/n)$, at most the area of the set $V_1 \cap B$ that contains it, edge s_1s_2 must have Euclidean length $O(D/n)$, and therefore also $d(s_1, s_2) = O(D/n)$ (larger than the Euclidean length by at most the constant factor $\frac{1}{\rho}$). For this distance to be a nonzero integer, n must be $O(D)$.
- Otherwise, p is on the boundary of V_1 , and equidistant (in Euclidean distance) from s_1 and some site s_3 which cannot be collinear with s_1s_2 . Therefore, the Euclidean distance from s_1 to p is at least half the Euclidean distance from s_1 to s_3 . Combining this inequality with the area of the triangle and the $\frac{1}{\rho}$ factor by which d can increase over Euclidean distance gives the bound $d(s_1, s_2) \cdot d(s_1, s_3) = O(D^2/n)$. It follows from Theorem 1 that $n = O(D^2/n)$ and therefore that $n = O(D)$. \square

The examples of $n \times n$ integer grids for the L_1 or L_∞ distance show that the assumption of strict convexity is necessary for this result.

4 Riemannian manifolds

In this section we prove a form of the Erdős–Anning theorem for two-dimensional complete Riemannian manifolds. These can be defined intrinsically (without respect to an embedding) as smooth manifolds equipped with a smoothly varying inner product structure on their tangent space. “Completeness” in this context means that all Cauchy sequences converge; for instance, puncturing the Euclidean plane by removing the origin would produce a space that is not complete. By the Nash embedding theorem [28] it is equivalent (and may be easier) to think of these as two-dimensional

surfaces, smoothly embedded into a Euclidean space of bounded dimension, with distance measured by the Euclidean length of curves on the surface. Standard examples of such spaces include the Euclidean plane itself, the surface of any smooth convex body in three dimensions such as a sphere, and the hyperbolic plane.

One complication in these spaces is that their usual analogues of straight lines, *geodesics*, are only locally shortest curves between their points: two or more points may belong to a common geodesic that does not contain the shortest curve between them. Indeed, in some cases a geodesic may cross itself or form a dense subset of its surface. For this reason, we will generally work with shortest curves (between some two points of the space) rather than geodesics. These curves may not be unique: for instance, for antipodal points on a sphere, there are infinitely many shortest curves, covering the whole sphere. By the Hopf–Rinow theorem [16], every complete Riemannian manifold has a shortest curve between every two points. Thus, these are geodesic metric spaces, and in particular the Lipschitz property of distances (Observation 1) applies to them.

We will not assume that the surfaces we consider are orientable. One way to parameterize a two-dimensional surface, without assuming orientability, is by its *Euler genus*, the number $2 - \chi$ where χ is the Euler characteristic. It is possible for a Riemannian manifold to have infinite genus, but (except for Example 7, which motivates this limitation) we will only work with surfaces of bounded genus.

4.1 Examples

We have the following analogue of Example 2:

Example 5. Consider any finite set of three or more points S on a unit sphere, no three of which belong to a great circle. Then each two points of S have a unique shortest curve which does not pass through other points of S . Perturb the sphere by placing a small smooth bump along each shortest curve, increasing the distance between its two points to a rational number without changing the other distances, and then scale the result to clear the denominators of these rational distances. The result is a complete Riemannian manifold of Euler genus zero with an arbitrary finite number of points at integer distances from each other.

It is necessary to assume that our Riemannian manifolds are complete, because of the following example:

Example 6. Consider the points coordinatized by two real numbers r and θ , with r positive and θ arbitrary, and with the standard locally Euclidean geometry of the polar coordinate system. This can be thought of as a cone with an infinite angle at its removed apex [31]. Its Euler genus is zero (topologically it is just an open halfplane). When two of its points have θ -coordinates that differ by at least π , their distance equals the sum of their r -coordinates (distances from the removed apex). Therefore, the points $\{(\frac{1}{2}, i\pi) \mid i \in \mathbb{Z}\}$ form an infinite set at unit distance from each other. They have no shortest curves, because any such curve would pass through the missing apex point.

As the next example shows, to obtain a generalization of the Erdos–Anning theorem to complete Riemannian manifolds, we will also need to assume bounded genus, and our bounds on numbers of points in integer distance sets will need to depend on the genus.

Example 7. For any n , one may form a complete Riemannian manifold from n spheres, connected by cutting out disks from pairs of spheres, attaching a cylindrical tube between the boundaries of the two disks, and smoothing the parts of the surface where the disks meet the tubes. This construction may be performed abstractly as a topological space; it is not necessary to embed the spheres and

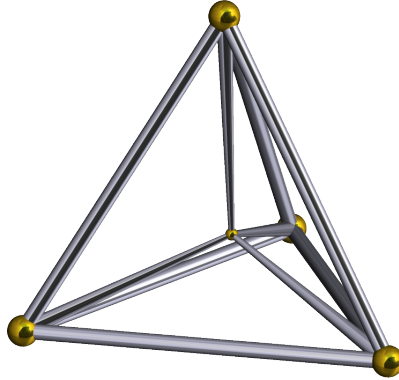


Figure 10: Five small spheres connected in pairs by cylindrical tubes. Smoothing the sphere-cube edges produces a complete Riemannian manifold. Public domain image from https://commons.wikimedia.org/wiki/File:Schlegel_wireframe_5-cell.png.

tubes into three-dimensional space. Let S consist of one point per sphere, for spheres small enough that all distances within one sphere are less than $\frac{1}{3}$; then by adjusting the lengths of all the tubes, all distances between points of S can be made equal to one. This construction produces arbitrarily large finite sets of points at unit distance from each other, with genus $O(n^2)$. Because they all have the same distance, no three of these points belong to a shortest curve.

The connected sum of an infinite sequence of examples of this type for $n = 4, 5, 6, \dots$, using tubes to connect the example for each n to the examples for $n - 1$ and $n + 1$, forms a single complete Riemannian manifold of infinite genus in which one can find arbitrarily large (but nevertheless finite) sets of points that are all at unit distance from each other.

Although the topological structure of this example is complicated, it can be embedded in a distance-preserving way into a Riemannian metric on \mathbb{R}^3 . For each n , choose the spheres and tubes of the n -point example to have a small enough radius that they can all be smoothly embedded within a unit ball of \mathbb{R}^3 , coiling the tubes to cause them to have the desired lengths. Form the connected sum of these examples as before and embed it smoothly in \mathbb{R}^3 using disjoint unit balls for each term in the connected sum. Thicken the resulting smoothly embedded surface S by a small amount (varying smoothly over the surface) chosen to be small enough that the thickened set remains smoothly embedded in \mathbb{R}^3 , and give the resulting thickened set a Riemannian metric that agrees with the metric on S (and the Euclidean distance of \mathbb{R}^3) in directions parallel to S , but that is longer in the direction perpendicular to S by a factor that varies smoothly from very large for points on S to one at the boundary of this thickened set. Then, for the remaining points of \mathbb{R}^3 , outside the thickened set, use the usual Euclidean distance. By choosing this perpendicular lengthening factor large enough, it is possible to ensure that escaping from S to the boundary of the thickened set takes more than unit distance, and that distances within S are preserved.

Richard Guy asked whether the *equilateral dimension* of Riemannian manifolds, the maximum cardinality of a set of points in the manifold for which all distances are one, can be bounded by a function of the dimension of the manifold [14]. A positive answer was known only for the case of complete Riemannian manifolds of bounded curvature [23]. Example 6 provides a counterexample for locally Euclidean and topologically simple but incomplete Riemannian 2-manifolds. Example 7 provides a counterexample for complete Riemannian 2-manifolds of unbounded genus and for topologically simple complete Riemannian 3-manifolds. On the other hand, our generalization of

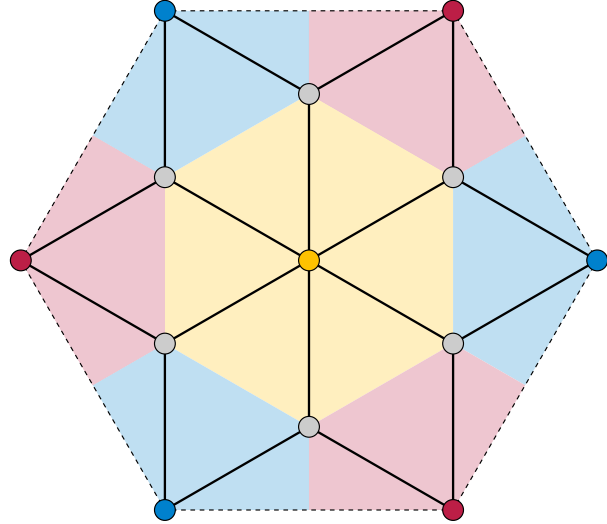


Figure 11: An embedding of $K_{3,6}$ with shortest-curve edges on a hexagonal torus (Example 8). The colors indicate the Voronoi diagram of the points on the three-vertex side of the bipartition.

the Erdős–Anning theorem to complete Riemannian 2-manifolds of bounded genus also provides a bound on the equilateral dimension of these manifolds, as a function of their genus (Corollary 20).

Our proof of the Erdős–Anning theorem for strictly convex distance functions relied on the non-planarity of $K_{3,3}$. For complete Riemannian manifolds of bounded genus we need to reach further for graphs that cannot be embedded, as the following example shows.

Example 8. Form a complete Riemannian manifold (the *hexagonal torus*) by gluing opposite edges of a Euclidean regular hexagon. The hexagon’s six vertices become two points of the torus (red and blue in Fig. 11). Let S consist of these two points and the center of the hexagon (yellow). Six points (gray) are equidistant from these three points. Connecting the three points of S by shortest curves to these six points embeds $K_{3,6}$ on the torus.

4.2 Voronoi cells

Our definitions of Voronoi diagrams for finite sets of sites, additively weighted Voronoi diagrams, and Voronoi cells apply to any metric space. We may define kernels and star-shaped sets, in complete Riemannian manifolds, by analogy to their Euclidean definitions. We define the *kernel* of a set S to be the set of points p such that, for every point $q \in S$, every shortest curve between p and q belongs to S . We define S to be *star-shaped* if its kernel is non-empty. Then we have the following analogue of Lemma 2. The proof, which depends only on the space being geodesic and on the Lipschitz property of distances, is unchanged.

Lemma 10. *For additively weighted Voronoi diagrams of complete Riemannian manifolds, every non-empty Voronoi cell is star-shaped with its site in its kernel.*

As before, we define a *degenerate site* to be a site that belongs to the Voronoi cell of another site, and a *non-degenerate site* to be a site that is not degenerate. To formulate an analogue of Lemma 3, we also need a definition of a ray in a complete Riemannian manifold. To do this, we use the *exponential map*. Given a point p of the manifold, and a vector v in the tangent space at p , the exponential map takes v to $\exp_p v$, another point in the manifold obtained by following a geodesic

from p for a length and direction specified by v . For Riemannian manifolds in general, this is defined only for a neighborhood of the origin in the tangent space, but for complete Riemannian manifolds it is defined for the whole tangent space. For any point p of the manifold, there is a number $r > 0$, the *injectivity radius*, such that the exponential map is an injection on vectors in the tangent space at p with radius $< r$, and not an injection for vectors with radius $\leq r$. The exponential map is a smooth topological equivalence (a diffeomorphism) between the disk of vectors of radius $< r$ and its image, a neighborhood of p in the manifold. We define a *ray* in a complete Riemannian manifold to be a set of the form

$$\{\exp_p cv \mid 0 < c\}$$

for a fixed choice of p (the starting point or *apex* of the ray) and v (a vector specifying the direction of the ray), and for all positive scalars c .

Another complication here is that, for convex distance functions, the intersection of a ray with a star-shaped set (having its apex in the kernel) is a line segment, and therefore a shortest curve. For complete Riemannian manifolds, a ray may continue through a star-shaped set past the last point for which it forms a shortest curve, or may even have a disconnected intersection with the set. It may also pass through some points of the manifold more than once. In a Voronoi diagram, we define the *Voronoi segment* of a ray, having one of its sites s_i as an apex, to be the union of all shortest curves from points in V_i to s_i that lie along the same ray.

Lemma 11. *Let s_i be a degenerate site of an additively weighted Voronoi diagram of a complete Riemannian manifold, with s_i belonging to the Voronoi cell V_j of another site s_j . Let R_j be a ray with apex s_j containing a shortest curve from s_i to s_j , and let R_i be a ray with apex s_i continuing in the same direction, away from s_i . Then either s_i is empty, or V_i is the intersection of R_i with the Voronoi segment of R_j .*

Proof. As in the proof of Lemma 3, if the weighted additive distance from s_i to s_j is less than the weighted distance from s_i to itself, then s_i does not belong to its own Voronoi cell and by Lemma 10 the cell must be empty. Otherwise, at s_i , the weighted distances to s_i and s_j are equal. Because the lengths of curves along rays increase at the same rate as distance traveled along a ray, the weighted lengths of curves along R_i and R_j remain equal for all points of R_i . At every point of the Voronoi segment, this weighted distance is the minimum distance to a site, and at every point of the past the endpoint of the Voronoi segment, it is not. \square

By repeatedly using Lemma 11 to replace the Voronoi cells of degenerate sites with supersets that are also Voronoi cells, until no more such replacements can be performed, we obtain an analogue of Corollary 4:

Corollary 12. *In an additively weighted Voronoi diagram of a complete Riemannian manifold, every point belongs to the Voronoi cell of at least one non-degenerate site.*

We also have the following analogue of Lemma 5:

Lemma 13. *A site s_i of an additively weighted Voronoi diagram of a 2-dimensional complete Riemannian manifold is non-degenerate if and only if it is an interior point of its cell V_i .*

The proof is the same as that for Lemma 5.

We interpreted Lemma 6 as stating that each ray with a non-degenerate site as its initial point passes through at most one boundary point of its Voronoi cell. This is not true for complete Riemannian manifolds, because rays can re-enter the Voronoi cell after the end of the Voronoi segment of the ray. On the other hand, a Voronoi segment of bounded length may have its endpoint

in the interior of a cell, and not pass through any boundary points of the cell. Nevertheless, we have the following analogue of Lemma 6:

Lemma 14. *Let s_i be a non-degenerate site of an additively weighted Voronoi diagram of a 2-dimensional complete Riemannian manifold, let L be a Voronoi segment in V_i having s_i as an endpoint, and let p be a point in the relative interior of L . Then p is interior to V_i .*

Proof. As in the proof of Lemma 6, the only other possibility is that there is some other Voronoi cell V_j also containing p , such that every neighborhood of p contains points of $V_j \setminus V_i$. Then the shortest curves from p to s_i and to s_j cannot follow the same ray from p ; otherwise, s_i would be degenerate (contradicting the assumption in the statement of the lemma) or s_j would be degenerate (contradicting the assumption that $V_j \setminus V_i$ is nonempty). For any point q past p on L , there would exist curves of equal length from q to s_i along L , and from q to s_j along L to p and then from p to s_j ; but because the curve to s_j turns at p it cannot be a shortest curve as it can be shortcut near p , so q is closer to s_j than s_i . But this would contradict the definition of L as a Voronoi segment. \square

4.3 Intersections of non-degenerate cells

Continuing the analogy from convex distance functions to Riemannian manifolds, we have the following analogue of Lemma 7. The proof is somewhat different because of the possibility that a point interior to a Voronoi cell may nevertheless be an endpoint of a Voronoi segment.

Lemma 15. *Let s_i and s_j be non-degenerate sites of an additively weighted Voronoi diagram for a 2-dimensional complete Riemannian manifold. Then the interior of V_i is disjoint from V_j , and vice versa.*

Proof. Suppose for a contradiction that there existed a point p interior to V_i that also belonged to V_j . Then any shortest curves ps_i and ps_j must be disjoint except for their shared endpoint, for otherwise one would be a subset of the other, and one of the two sites would belong to the Voronoi cell of the other, contradicting the assumption that both are non-degenerate. Because p is interior to V_i , there must be some point $q \neq p$ on segment ps_j that also belongs to V_i . But by the Lipschitz property of distances, the weighted distance to s_j decreases more quickly along curve pq than the weighted distance to s_i , a contradiction. \square

Continuing the analogy, we have:

Lemma 16. *Let s_i and s_j be distinct non-degenerate sites of an additively weighted Voronoi diagram of a 2-dimensional complete Riemannian manifold, and let p and q be distinct points of V_i and V_j respectively. Then line segments (or arcs) ps_i and qs_j are disjoint.*

Proof. Otherwise, one of these two segments would contain a point in the relative interior of the other segment or arc. By Lemma 14 this point would be interior to its Voronoi cell, contradicting Lemma 15. \square

To formulate an analogue of Lemma 9 we must first account for examples like Example 8 in which triples of Voronoi cells have more than two points of intersection, corresponding to drawings of graphs $K_{3,a}$ with $a > 2$ and with all edges drawn as shortest curves.

Lemma 17. *On a surface of Euler genus g , the maximum number a such that $K_{3,a}$ can be drawn without crossings on the surface is at most $2g + 2$.*

Proof. In any drawing of $K_{3,a}$ on any surface, all faces of the drawing have at least four sides, and each edge forms exactly two sides of faces (not necessarily distinct). Therefore, if V , E , and F are the sets of vertices, edges, and faces of the drawing, we have

$$2|E| \geq 4|F|.$$

We also have

$$|V| - |E| + |F| \geq 2 - g$$

by the definition of the Euler characteristic, where the inequality comes from the fact that we are not assuming that the faces of the drawing are disks. Using the first inequality to eliminate $|F|$ from the second gives

$$|V| - \frac{1}{2}|E| \geq 2 - g.$$

or equivalently

$$|E| \leq 2|V| + 2g - 4.$$

The graph $K_{3,a}$ has $|V| = 3 + a$ and $|E| = 3a$. In order to have $3a \leq 2(3 + a) + 2g - 4$, we must have $a \leq 2g + 2$. \square

This is a known result; see, e.g., Bouchet [5], who credits the complete characterization of the genus of complete bipartite graphs to several works of Ringel from the mid-1960s. The Euler genus zero case of this lemma is the fact that $K_{3,3}$ is non-planar, while the Euler genus two case includes the fact that $K_{3,7}$ cannot be drawn on a torus. In these cases, the lemma is tight: $K_{3,2}$ is planar and Example 8 shows that $K_{3,6}$ is toroidal.

Finally, this allows us to bound the number of triple intersections of Voronoi cells:

Lemma 18. *Let s_i , s_j , and s_k be three sites of an additively weighted Voronoi diagram of a 2-dimensional complete Riemannian manifold of Euler genus g , with none of the three sites belonging to any shortest curve between the other two sites. Then $V_i \cap V_j \cap V_k$ consists of at most $2g + 2$ points.*

Proof. Without loss of generality we may consider that these are the only three sites of the Voronoi diagram, because adding more sites can only reduce the points in $V_i \cap V_j \cap V_k$ by causing some of those points to belong to Voronoi cells of other sites. By Lemma 14 and Lemma 15, the whole space is covered by the cells of non-degenerate sites, with disjoint interiors. We distinguish cases by how many of the three given sites are non-degenerate:

- Suppose that there is only one non-degenerate site, without loss of generality s_i . Then, V_i is the whole space, and V_j and V_k lie on Voronoi segments of s_i . These segments are distinct (else one of s_j and s_k would lie on a shortest curve from s_i to the other). A point p interior to one Voronoi segment cannot belong to another Voronoi segment, because if it did the points past p on the first segment would have an equally short curve to s_i that follows the first segment to p and then the second curve to s_i , but such a non-geodesic curve cannot be a shortest curve (it could be made shorter by adding a small shortcut near p). Therefore, in this case the only point of intersection can be a shared endpoint of the Voronoi segments of s_i that contain s_j and s_k , giving $|V_i \cap V_j \cap V_k| \leq 1$.
- In the next case, there are two non-degenerate sites, without loss of generality s_i and s_j . Because it is degenerate, s_k belongs to at least one of their Voronoi cells, without loss of generality V_i . By Lemma 3, V_k is the intersection of a ray from s_k with a Voronoi segment of V_i . By Lemma 14 and Lemma 15, only the endpoint of this Voronoi segment can belong to V_j . Thus, in this case, $|V_i \cap V_j \cap V_k| \leq 1$ again.

- In the remaining case, all three sites are non-degenerate. In particular, none of them belong to $V_i \cap V_j \cap V_k$. Consider the system of Voronoi segments connecting each site to each point of $V_i \cap V_j \cap V_k$. These line segments cannot intersect except at shared endpoints, so they form a planar drawing of a complete bipartite graph with the three sites on one side of its bipartition and the points of $V_i \cap V_j \cap V_k$ on the other side. By Lemma 17, $|V_i \cap V_j \cap V_k| \leq 2g + 2$. \square

4.4 Erdős–Anning theorems for Riemannian manifolds

Theorem 4. *Let s_1 , s_2 , and s_3 be three points of a 2-dimensional complete Riemannian manifold of Euler genus g , with distance function d . Suppose also that there is no shortest curve containing all three of these points. Then the number of points that can have integer distances to all three of s_1 , s_2 , and s_3 is $O((g+1) \cdot d(s_1, s_2) \cdot d(s_1, s_3))$.*

Except for the factor of g coming from Lemma 18, the proof is the same as for Theorem 1. For this theorem, the possibility that all triples of points lie on shortest curves (preventing the theorem from being applied) corresponds to the possibility of all points being collinear in the Euclidean plane or for convex distance functions. It is a strengthening of the more obvious generalization of collinearity, that all points of S lie on a common geodesic:

Lemma 19. *Let S be a set of three or more points of a complete Riemannian manifold such that each three points of S belong to a shortest curve. Then S is a subset of a geodesic, and every shortest curve between pairs of points in S lies along this geodesic.*

Proof. Let s_1 be any of the points, and consider the system of rays containing shortest curves to all the other points. Suppose for a contradiction that two rays R_2 and R_3 in this system of rays contain shortest curves from s_1 to points s_2 and s_3 in S , and that these two rays are distinct and non-opposite. Then if s_1 were on a shortest path from s_2 to s_3 , then a shortest curve from s_2 to s_3 would follow R_2 from s_2 to s_1 and then follow R_3 from s_1 to s_3 . This cannot happen, because a shortest curve that turns from one ray to another at s_1 could be shortcut by a different curve in a neighborhood of s_1 . Alternatively, if s_2 were on a shortest curve from s_1 to s_3 , then we could get a shortest curve from s_1 to s_3 that follows R_2 from s_1 to s_2 , turns at s_2 , and then continues along the R_3 from s_2 to s_3 , again an impossibility. The case that s_3 is on a shortest curve from s_1 to s_2 is symmetric. So none of the three points can be the middle point of a shortest curve containing all three points. This contradiction to the assumption of the lemma implies that rays R_2 and R_3 cannot exist, and that the system of rays contains either a single ray or two opposite rays. In either case, these two rays, and therefore all points of S , lie on a single geodesic.

If some two points s_2 and s_3 had a shortest curve that did not lie along this geodesic, then we could apply this same argument to the rays at s_2 containing the shortest curve to s_1 (along the geodesic through all points of S) and the ray containing the shortest curve from s_2 to s_3 (not along this geodesic), obtaining the same contradiction. Therefore all shortest curves lie on the same geodesic. \square

The conclusion of this lemma cannot be strengthened to state that each pair of points in S has a unique shortest curve. For instance, consider an even number of points equally spaced on the equator of a sphere. In this example, each point has two shortest curves to its opposite point. A set of points whose shortest curves all lie on a single geodesic might still not have the property that each three points belong to a shortest curve: consider, for instance, three equally spaced points on the equator of a sphere.

Combining Theorem 4 with Lemma 19 gives us the following generalization of the Erdős–Anning theorem:

Theorem 5. *If a set S of points of a 2-dimensional complete Riemannian manifold of bounded genus has the property that all distances between points of S are integers, then either S is finite or there is a single geodesic of the manifold containing all points of S and connecting each pair of points by a shortest curve.*

We also have the following diameter bound, weaker than in the Euclidean or convex distance function case:

Theorem 6. *If a set S of points of a 2-dimensional complete Riemannian manifold of bounded genus g has integer distances and diameter D , then $|S| = O(gD^2)$.*

Proof. If S has three points not all on a single shortest curve, this follows from Theorem 4. Otherwise, the points all have shortest curves along a geodesic. Let C be a shortest curve of length D between some two points of S . If C covers all points of S , there are at most $D + 1$ points. Otherwise, let s_1 and s_2 be the two endpoints of C , and let s_3 be any point not covered by C . For s_1 , s_2 , and s_3 to be part of a shortest curve, the curve must have s_1 and s_2 as endpoints, for otherwise we would have a shortest curve that includes a segment from s_1 to s_2 , causing it to be longer than D . In this case, the only possibility is that s_1 and s_2 have two shortest paths, and are at distance D from each other along a geodesic of length $2D$, so there are at most $2D$ points in S . \square

Corollary 20. *The equilateral dimension of a 2-dimensional complete Riemannian manifold of bounded genus g is $O(g)$.*

5 Convex surfaces

In this section we extend our results on Riemann manifolds to non-smooth surfaces of non-negative curvature. The restriction to non-negative curvature is motivated by Example 6, which shows that even a single cone point of negative curvature can be an obstacle to Erdős–Anning theorems. For concreteness, in this section we usually define a *convex surface* to mean the boundary of a convex subset of \mathbb{R}^3 with nonempty interior. However, we also allow a special case, which can be thought of as the limit of convex cylinders as the cylinder height goes to zero: the double covering of a convex subset K of \mathbb{R}^2 , obtained by gluing two copies of K at corresponding boundary points. For instance, the Euclidean plane is a convex surface in the first of these two senses: it is the boundary of a halfspace. By results of Aleksei Pogorelov, a more abstract class of non-smooth convex manifolds, topologically equivalent to a sphere and with total Gaussian curvature 4π , can be characterized as being either boundaries of convex bounded subsets of \mathbb{R}^3 or double covers of convex bounded subsets of \mathbb{R}^2 [8]. We include double covers in our definition of convex surfaces to be consistent with this result of Pogorelov, but we do not require the convex sets from which they are defined to be bounded. We measure the distance on a convex surface as the infimum of lengths of curves on the surface. By a compactness argument, each pair of points on the surface can be connected by a curve of length equal to this distance, so this is a geodesic metric space [26], and we can apply arguments involving the Lipschitz property of distances. Every convex surface, in the sense described here, is topologically a disk (like the Euclidean plane), a sphere (like a geometric sphere, polyhedron, or double-covered topological disk), or an annulus (like the boundary of an infinite cylinder).

The boundary of a (bounded) solid cone (Fig. 12) exhibits several of the common geometric features of a convex surface. The base of the cone is a flat disk; the sides of the cone have a flat surface metric (locally isometric to a subset of the Euclidean plane) even though they are curved in three-dimensional space. The circle where the base meets the sides is non-smooth; each point has a neighborhood that approaches a Euclidean metric (equivalent to that of a folded piece of paper)

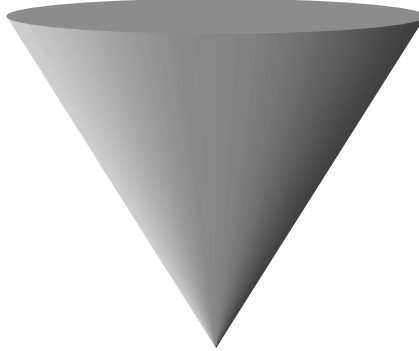


Figure 12: A solid cone

in the limit. The apex of the cone, however, is not Euclidean, even in the limit: it has a positive angular deficiency that can be measured by comparing the radius and circumference of small metric disks around it. The total curvature of this surface is 4π , by the Gauss–Bonnet theorem, but in this case this curvature is concentrated at the cone point (where it equals the angular deficit of this point) and along the circle where the base and sides meet.

In general, when a shortest curve on a convex surface passes through a locally Euclidean point, it must pass straight through it, in the local Euclidean geometry of a neighborhood of a point. A curve that does not do this could be shortcut to bypass the point. It is not possible for a shortest curve to pass through a cone point (any point of positive angular deficiency): any curve through such a point can be shortcut. Thus, we need only consider such points as endpoints of shortest curves, not as their interior points.

Lemma 21. *For every point p on a convex surface, the disks of radius r centered on that point, in the limit as $r \rightarrow 0$, approach a cone for which p either has angular deficit zero (p is locally Euclidean) or a well-defined positive angular deficit (p is locally a cone point).*

Proof. For a point p on a convex surface, let $C_r(p)$ denote the cone formed by positive combinations of p with the points at distance r from p on the surface. Then C_r is monotone in r : for $r' < r$, $C'_r(p) \supset C_r(p)$, by convexity. By compactness of the space of cones at a point p , in the limit as r goes to zero, these cones approach a limiting cone; call this limit $C_0(p)$. Let B be the curve obtained by intersecting the boundary of $C_0(p)$ with a unit sphere centered at p . Then B is convex, and lies in a half-sphere, again by convexity of the convex surface. Thus, its length is at most 2π . If it is exactly 2π , then p is locally Euclidean; otherwise, it is locally equivalent to a cone point with deficit equal to the difference between 2π and the length of B . \square

5.1 Voronoi diagrams and their properties

For convex surfaces, we define star-shaped sets, additively weighted Voronoi diagrams, rays, Voronoi segments, and degenerate and non-degenerate sites in the same way as for Riemannian manifolds. One small difference is that a ray can terminate, by hitting a cone point. Because every point is either locally a cone point (with no geodesics through it) or locally Euclidean (with all geodesics passing straight through it) the behavior of geodesics on convex surfaces is much the same as for Riemannian manifolds: the cone points do not affect them at all, and the non-smooth geometry of the surface at the remaining points does not affect our use of this geometry to prove properties of these spaces. We have the following results, analogous to those for Riemannian manifolds, with the same proofs:

Lemma 22. *For additively weighted Voronoi diagrams of convex surfaces, every non-empty Voronoi cell is star-shaped with its site in its kernel.*

Proof. Same as for Lemma 2 and Lemma 10. \square

Lemma 23. *Let s_i be a degenerate site of an additively weighted Voronoi diagram of a convex surface, with s_i belonging to the Voronoi cell V_j of another site s_j . Let R_j be a ray with apex s_j containing a shortest curve from s_i to s_j , and let R_i be a ray with apex s_i continuing in the same direction, away from s_i . Then either s_i is empty, or V_i is the intersection of R_i with the Voronoi segment of R_j .*

Proof. Same as for Lemma 11. \square

Corollary 24. *In an additively weighted Voronoi diagram on a convex surface, every point belongs to the Voronoi cell of at least one non-degenerate site*

Lemma 25. *A site s_i of an additively weighted Voronoi diagram on a convex surface is non-degenerate if and only if it is an interior point of its cell V_i .*

Proof. Same as for Lemma 5 and Lemma 13. \square

Lemma 26. *Let s_i be a non-degenerate site of an additively weighted Voronoi diagram on a convex surface, let L be a Voronoi segment in V_i having s_i as an endpoint, and let p be a point in the relative interior of L . Then p is interior to V_i .*

Proof. Same as for Lemma 14, which depends only on the local Euclidean geometry of the surface at an interior point of a shortest curve to argue that no curve that bends at such a point can be shortest. Here we are using the fact that no interior point of a shortest curve can be a cone point. \square

Lemma 27. *Let s_i and s_j be non-degenerate sites of an additively weighted Voronoi diagram on a convex surface. Then the interior of V_i is disjoint from V_j , and vice versa.*

Proof. Same as for Lemma 15. \square

Lemma 28. *Let s_i and s_j be distinct non-degenerate sites of an additively weighted Voronoi diagram on a convex surface, and let p and q be distinct points of V_i and V_j respectively. Then line segments (or arcs) ps_i and qs_j are disjoint.*

Proof. Same as for Lemma 16. \square

Lemma 29. *Let s_i , s_j , and s_k be three sites of an additively weighted Voronoi diagram on a convex surface, with none of the three sites belonging to any shortest curve between the other two sites. Then $V_i \cap V_j \cap V_k$ consists of at most two points.*

Proof. Same as Lemma 18, noting that convex surfaces have Euler genus zero. \square

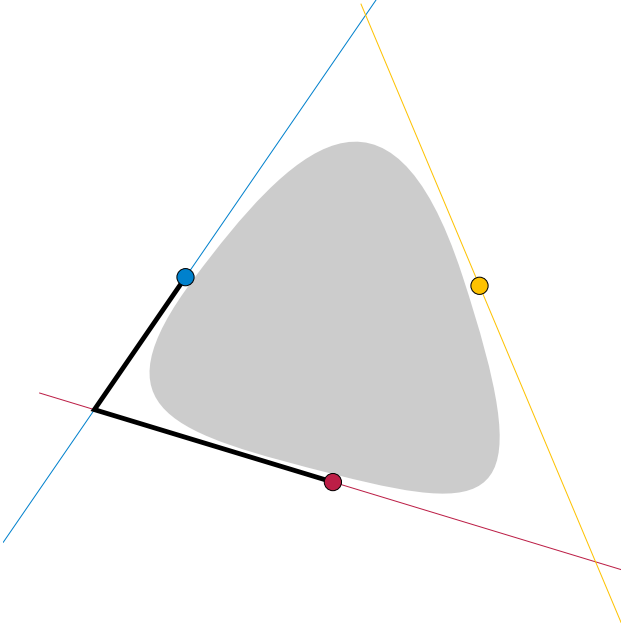


Figure 13: Lemma 31: a short path connecting two of three points separated by a convex set

5.2 Erdős–Anning theorems for convex surfaces

Theorem 7. *Let s_1 , s_2 , and s_3 be three points of a convex surface, with distance function d . Suppose also that there is no shortest curve containing all three of these points. Then the number of points that can have integer distances to all three of s_1 , s_2 , and s_3 is $O(d(s_1, s_2) \cdot d(s_1, s_3))$.*

Proof. Same as for Theorem 1 and Theorem 4, substituting the properties of additive Voronoi diagrams for convex surfaces in place of the corresponding properties of the diagrams for convex distance functions and Riemannian manifolds. \square

Lemma 30. *Let S be a set of three or more points of a convex surface such that each three points of S belong to a shortest curve. Then S is a subset of a geodesic, and every shortest curve between pairs of points in S lies along this geodesic.*

Proof. Same as for Lemma 19, again substituting the properties of Voronoi diagrams on these surfaces. \square

Theorem 8. *If a set S of points of a convex surface has the property that all distances between points of S are integers, then either S is finite or all triples of points in S are subsets of shortest curves along a single geodesic.*

Proof. Same as for Theorem 5, again substituting the properties of Voronoi diagrams on these surfaces. \square

Our diameter bound seems unlikely to be tight. It uses the following preliminary lemmas.

Lemma 31. *Suppose that three given points in \mathbb{R}^d are disjoint from an open convex set U . Then two of the points can be connected by a curve disjoint from U of length at most twice their Euclidean distance.*

Proof. Consider the plane containing the three points; if U does not intersect this plane then the points can be connected directly. Within this plane draw a line through each point, disjoint from U . The three lines form a triangle or unbounded three-sided region containing U ; if all three points lie on its sides, one of its internal angles is $\geq 60^\circ$, and the curve connecting two points through this angle has length at most twice the distance between the points (Fig. 13; worst case: U is an equilateral triangle and the three points are its edge midpoints). If one of the three points is not on a side of the region containing U , it can see the entire line through another of the points, and be connected directly to that point. \square

Lemma 32. *If n points on a convex surface have diameter D then some two of the points have geodesic distance $O(D/\sqrt{n})$.*

Proof. Let the set of points be S , and let the convex surface be the boundary of a set K (or the double cover of a set K), embedded in \mathbb{R}^3 . By assumption, S lies within a ball B of radius D in \mathbb{R}^3 . Subdivide the ball by a grid of cubes, of side length $O(D/\sqrt{n})$, positioned so that none of the given points lies on a cube boundary, and let \square denote the set of cubes in this grid whose intersection with $B \cap K$ is non-empty and includes at least one non-vertex point of the cube. Each point in S is contained in at least one cube $C \in \square$. This cube C must touch (at least at a corner) a grid cube that is outside \square , because if all eight cubes corner-adjacent to C belonged to \square , the intersection points of these eight cubes with $B \cap K$ would have a convex hull that entirely encloses C , preventing C from containing any boundary points of K . Therefore, C is within $O(1)$ grid positions of a boundary square of the union of cubes $\cup \square$. But $\cup \square$ is orthogonally convex – any axis-parallel line can cross only two boundary squares (one in each direction) – so it has $O(n)$ boundary squares. Therefore there are also $O(n)$ cubes near these squares that contain points of S . By choosing the grid size appropriately, we can adjust the constant factors in this $O(n)$ bound and ensure that fewer than $n/2$ cubes contain points of S . With this adjustment, some cube $C \in \square$, of side length $O(D/\sqrt{n})$, contains at least three points of S . We consider two cases:

- If the convex surface is non-degenerate (it bounds a convex set with non-empty interior), then by Lemma 31, two of these three points are connected by a path in space, disjoint from the interior of the given convex set, of length $O(D/\sqrt{n})$, and hence are at geodesic distance $O(D/\sqrt{n})$ on the convex surface.
- Otherwise, the convex surface is a double-covered two-dimensional convex set, two of the three points are on the same side of the double cover, and these two points can be connected directly within C by a geodesic segment of length $O(D/\sqrt{n})$.

In either case, we have two points at geodesic distance $O(D/\sqrt{n})$. \square

The example of a square grid of $\sqrt{n} \times \sqrt{n}$ points on a flat plane, scaled to have diameter D , shows that Lemma 32 is tight.

Theorem 9. *If a set S of points of a convex surface has integer distances and diameter D , then $|S| = O(D^{4/3})$.*

Proof. Let n be the size of S , and let its two closest such points be p and q , with distance $O(D/\sqrt{n})$ by Lemma 32. We distinguish two cases:

- Suppose that all triples of points in S that include both p and q belong to shortest curves. Each point in S must belong either to a ray from p through q or a ray from q through p , with the ray containing a shortest curve from p to q . Further, this shortest curve (and hence these

two rays) must be unique, for if there were two shortest curves between p and q , one of them could be combined with part of a shortest curve from p or q to a third point r to form a shortest curve that passes through q or p at a non-straight angle, an impossibility. Thus, two rays contain all remaining points in S , and these points lie at integer spacing along these two rays, giving $O(D)$ points in S in total.

- Otherwise, some point r does not lie on a shortest curve with p and q . By Theorem 7, there can be $O(D^2/\sqrt{n})$ points in S . That is, $n = O(D^2/\sqrt{n})$. Multiplying both sides by \sqrt{n} and taking the $2/3$ power gives the result. \square

6 Discussion

We have shown that integer-distance point sets are finite or collinear in three broad classes of metric spaces each generalizing Euclidean distance in the plane. The next natural direction to look for a further extension of these results is in higher dimensions. Erdős and Anning state without proof that their results extend to d -dimensional Euclidean space [1]. However, the obvious attempt to generalize our proof to higher dimensions, by using intersection patterns of $(d+1)$ -tuples of Voronoi cells, does not work for convex distance functions: there exist three-dimensional convex distance functions for which some 4-tuple of points is equidistant from arbitrarily many other points [17]. For Riemannian manifolds, the theorem does not generalize, as Example 7 shows. Nevertheless, it would be interesting to study similar questions for higher-dimensional uniform metrics, such as hyperbolic space. It would also be of interest to strengthen the bound on diameter in Theorem 6 and Theorem 9.

References

- [1] Norman H. Anning and Paul Erdős. Integral distances. *Bulletin of the American Mathematical Society*, 51(8):598–600, 1945. doi:10.1090/S0002-9904-1945-08407-9.
- [2] Peter F. Ash and Ethan D. Bolker. Generalized Dirichlet tessellations. *Geometriae Dedicata*, 20(2):209–243, 1986. doi:10.1007/BF00164401.
- [3] Jeffrey M. Augenbaum and Charles S. Peskin. On the construction of the Voronoi mesh on a sphere. *Journal of Computational Physics*, 59(2):177–192, 1985. doi:10.1016/0021-9991(85)90140-8.
- [4] Mikhail Bogdanov, Olivier Devillers, and Monique Teillaud. Hyperbolic Delaunay complexes and Voronoi diagrams made practical. *Journal of Computational Geometry*, 5(1):56–85, 2014. doi:10.20382/JOCG.V5I1A4.
- [5] André Bouchet. Orientable and non orientable genus of the complete bipartite graph. *Journal of Combinatorial Theory, Series B*, 24:24–33, 1978. doi:10.1016/0095-8956(78)90073-4.
- [6] L. Paul Chew and Robert L. (Scot) Drysdale, III. Generalization of Voronoi diagrams in the plane. *SIAM Journal on Computing*, 10(1):73–87, 1981. doi:10.1137/0210006.
- [7] L. Paul Chew and Robert L. (Scot) Drysdale, III. Voronoi diagrams based on convex distance functions. In Joseph O'Rourke, editor, *Proceedings of the First Annual Symposium on Computational Geometry, Baltimore, Maryland, USA, June 5–7, 1985*, pages 235–244. Association for Computing Machinery, 1985. doi:10.1145/323233.323264.

[8] Robert Connelly. *Convex Polyhedra* by A. D. Alexandrov. *SIAM Review*, 48(1):157–160, March 2006. URL: <https://www.jstor.org/stable/204537>, doi:10.1137/SIREAD00004800000100014900001.

[9] Olivier Devillers, Stefan Meiser, and Monique Teillaud. The space of spheres, a geometric tool to unify duality results on Voronoi diagrams. In *Proceedings of the 4th Canadian Conference on Computational Geometry (CCCG '92)*, pages 263–268, 1992. URL: <https://cccg.ca/proceedings/1992/Paper43.pdf>.

[10] David Eppstein. *Forbidden Configurations in Discrete Geometry*. Cambridge University Press, 2018. doi:10.1017/9781108539180.

[11] Paul Erdős. Integral distances. *Bulletin of the American Mathematical Society*, 51:996, 1945. doi:10.1090/S0002-9904-1945-08490-0.

[12] Leonhard Euler. Fragmenta arithmeticæ ex Adversariis mathematicis deprompta, C: Analysis Diophantæa. In *Opera postuma*, volume I, pages 204–263. Eggers, Petropolis, 1862. Theorem 65, p. 229. URL: <https://scholarlycommons.pacific.edu/euler-works/806/>.

[13] Rachel Greenfeld, Marina Iliopoulou, and Sarah Peluse. On integer distance sets. Electronic preprint arxiv:2401.10821, 2024.

[14] Richard K. Guy. An olla-podrida of open problems, often oddly posed. *The American Mathematical Monthly*, 90(3):196–200, 1983. doi:10.2307/2975549.

[15] Heiko Harborth. Integral distances in point sets. In *Charlemagne and his Heritage: 1200 Years of Civilization and Science in Europe, Vol. 2 (Aachen, 1995)*, pages 213–224. Brepols, Turnhout, Belgium, 1998. doi:10.1484/M.STHS-EB.4.2017040.

[16] H. Hopf and W. Rinow. Ueber den Begriff der vollständigen differentialgeometrischen Fläche. *Commentarii Mathematici Helvetici*, 3(1):209–225, 1931. doi:10.1007/BF01601813.

[17] Christian Icking, Rolf Klein, Ngoc-Minh Lê, and Lihong Ma. Convex distance functions in 3-space are different. *Fundamenta Informaticæ*, 22(4):331–352, 1995. doi:10.3233/FI-1995-2242.

[18] Menelaos I. Karavelas and Ioannis Z. Emiris. Root comparison techniques applied to computing the additively weighted Voronoi diagram. In *Proceedings of the Fourteenth Annual ACM-SIAM Symposium on Discrete Algorithms, January 12–14, 2003, Baltimore, Maryland, USA*, pages 320–329. ACM and SIAM, 2003. URL: <https://dl.acm.org/citation.cfm?id=644108.644161>.

[19] Michael Kleber. Encounter at far point. *Mathematical Intelligencer*, 1:50–53, 2008. doi:10.1007/BF02985756.

[20] Tobias Kreisel and Sascha Kurz. There are integral heptagons, no three points on a line, no four on a circle. *Discrete & Computational Geometry*, 39(4):786–790, 2008. doi:10.1007/s00454-007-9038-6.

[21] Ngoc-Minh Lê. On non-smooth convex distance functions. *Information Processing Letters*, 63(6):323–329, 1997. doi:10.1016/S0020-0190(97)00136-1.

[22] Greg Leibon and David Letscher. Delaunay triangulations and Voronoi diagrams for Riemannian manifolds. In Siu-Wing Cheng, Otfried Cheong, Pankaj K. Agarwal, and Steven Fortune, editors, *Proceedings of the Sixteenth Annual Symposium on Computational Geometry, Clear Water Bay*,

Hong Kong, China, June 12–14, 2000, pages 341–349. ACM, 2000. doi:10.1145/336154.336221.

- [23] Jeremy Mann. Equilateral dimension of Riemannian manifolds with bounded curvature. *Rose-Hulman Undergraduate Mathematics Journal*, 14(1):Article 8, 2013. URL: <https://scholar.rose-hulman.edu/rhumj/vol14/iss1/8/>.
- [24] M. Mazón and T. Recio. Voronoi diagrams on orbifolds. *Computational Geometry: Theory & Applications*, 8(5):219–230, 1997. doi:10.1016/S0925-7721(96)00017-X.
- [25] R. E. Miles. Random points, sets and tessellations on the surface of a sphere. *Sankhyā, Series A*, 33:145–174, 1971. URL: <https://www.jstor.org/stable/25049720>.
- [26] S. B. Myers. Arcs and geodesics in metric spaces. *Transactions of the American Mathematical Society*, 57:217–227, 1945. doi:10.1090/S0002-9947-1945-0011792-9.
- [27] Hyeon-Suk Na, Chung-Nim Lee, and Otfried Cheong. Voronoi diagrams on the sphere. *Computational Geometry, Theory and Applications*, 23(2):183–194, 2002. doi:10.1016/S0925-7721(02)00077-9.
- [28] John Nash. The imbedding problem for Riemannian manifolds. *Annals of Mathematics, 2nd Ser.*, 63(1):20–63, 1956. doi:10.2307/1969989.
- [29] Frank Nielsen and Richard Nock. Hyperbolic Voronoi diagrams made easy. In Bernady O. Apduhan, Osvaldo Gervasi, Andrés Iglesias, David Taniar, and Marina L. Gavrilova, editors, *Proceedings of the 2010 International Conference on Computational Science and Its Applications, ICCSA 2010, Fukuoka, Japan, March 23–26, 2010*, pages 74–80. IEEE Computer Society, 2010. doi:10.1109/ICCSA.2010.37.
- [30] József Solymosi. Note on integral distances. *Discrete & Computational Geometry*, 30(2):337–342, 2003. doi:10.1007/s00454-003-0014-7.
- [31] Matthias Weber, David Hoffman, and Michael Wolf. An embedded genus-one helicoid. *Proceedings of the National Academy of Sciences*, 102(46):16566–16568, 2005. doi:10.1073/pnas.0508008102.